

Analysis of Microstrip Open-End and Gap Discontinuities
in a Substrate-superstrate Configuration

Hung-Yu Yang*, Nicolaos G. Alexopoulos*, David R. Jackson**

* Elec. Engin. Dept., University of California, Los Angeles, CA 90024
** Elec. Engin. Dept., Houston University, University Park, TX 77004

Abstract

A study of microstrip open-end and gap discontinuities in a two-layer structure is presented. The analysis is based on the method of moments solution of a full wave integral equation. A combination of semi-infinite modes and subdomain modes is used. The transverse dependence of the expansion functions is obtained through a two dimensional infinite analysis. A parametric study of the material effects on the radiation and surface wave losses, and the fringing fields at the discontinuities is also performed. The analysis has been checked with good agreement in the limiting case with the quasi-static method.

I. Introduction

Microstrip open-end and gap discontinuities are useful in the design of matching stubs and coupled filters. In recent years, layered integrated structures have found various applications in MIC and printed circuit antennas, especially for monolithic applications. Therefore, the design data for open-end and gap discontinuities in layered structures would be useful. In this paper, microstrip open-end and gap discontinuities in a substrate-superstrate configuration (Figs. 1 and 2) will be considered. The characterization of these discontinuities for a single layer has been performed quite extensively in the past. Quasi-static methods based on solving Poisson's equation have been applied for low frequency applications [1] - [4]. For higher frequencies, models based on a rigorous dynamic analysis are required. A spectral-domain approach [5] - [6] has been used to characterize the discontinuity problems with an enclosed waveguide housing. Therefore, the radiation and surface wave effects are not considered in that approach. A dynamic method based on solving integral equations by the method of moments has recently been applied to the modeling of microstrip open-end and gap discontinuities for a single layer case [7] - [8]. This analysis takes into account all of the physical effects including radiation, surface waves, and dominant as well as higher-order mode coupling. In [7], a finite but long microstrip line with a δ -gap source is used, which usually requires many basis functions and is numerically inefficient. In [8], a more efficient method is used with a combination of the entire domain and subdomain modes. However, from the discussion presented in [8], it seems that the method does not provide reliable results for the capacitance calculation. In this paper, a revised analysis of [8] is performed and applied to two layer structures.

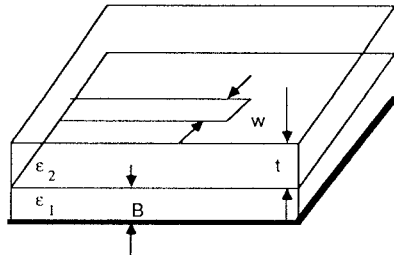


Figure 1. An open-end microstrip line in a two-layer structure.

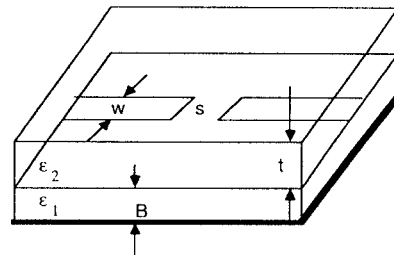


Figure 2 Microstrip gap in a two-layer structure

For the transverse dependence of the expansion functions in the method of moments, it is possible that with sufficiently high frequencies, a simple Maxwellian or pulse function used in [7] and [8] may not be a good approximation when the dominant mode is not TEM-like. Therefore in this analysis, the transverse dependence of the longitudinal current is obtained by a two dimensional infinite line analysis where three modified cos-Maxwellian functions are used [9]. The open-end discontinuity is characterized through the open-end capacitance or excess length (electrical length - physical length) which is mainly due to the fringing electrical field. When radiation loss is considered, a conductance should also be included in the equivalent circuit model. The gap discontinuity can be modeled as a π network with two capacitances (see Fig. 3). The loss mechanism can be included by adding two conductances in the equivalent circuit. The material effects of the layers on the radiation and surface wave loss, and the fringing fields at the discontinuities, will also be discussed.

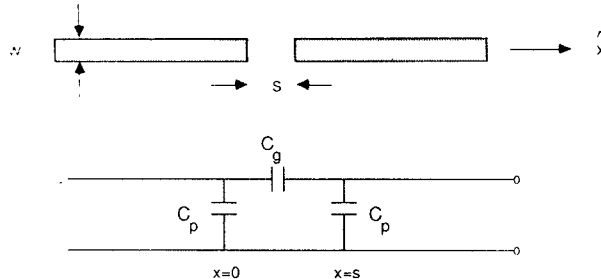


Figure 3. Microstrip gap discontinuity and its equivalent circuit.

II. Analysis

The transverse current has been found in the past to be a few orders smaller than the longitudinal current for width $< 0.1\lambda_0$ [10], and is neglected for simplicity. Under such circumstances, an integral equation for an open-end case can be formulated in terms of the longitudinal electric field on the microstrip.

$$E_x(x, y, z) = \int_{-\infty}^0 \int_{-w/2}^{w/2} G_{xx}(x, y, z|x_s, y_s, z_s) J_x(x_s, y_s) dy_s dx_s \quad (1)$$

where E_x is the electric field due to the current at $z = z_s$. The Green's function G_{xx} is the field E_x at (x, y, z) due to an \hat{x} directed delta source at (x_s, y_s, z_s) and is given in [11]. In the method of moment procedure, the unknown current distribution is expanded in terms of a set of known functions. An efficient way is to use the current on an infinite line to represent the fundamental guided wave mode of the microstrip line, and to use subdomain modes (piecewise sinusoidal modes or PWS modes) to describe the current behavior in the vicinity of the discontinuities [8]. Since the microstrip open end is a special case of the gap discontinuity, the formulation in the following will be for the gap case. Referring to Fig. 3, the current in the microstrip can be expanded as

$$J_x(x, y) = f(x) J_f(y) \quad (2)$$

with

$$f(x) = e^{-jk_m x} - \Gamma e^{jk_m x} + \sum_{n=1}^N I_{n1} f_n(x) \quad \text{for } x \leq 0, \quad (3)$$

$$f(x) = T e^{-jk_m(x-s)} + \sum_{n=1}^N I_{n2} g_n(x) \quad \text{for } x \geq s, \quad (4)$$

and

$$J_f(y) = \frac{a_0 + a_1 \cos(\frac{2\pi}{w}y) + a_2 \cos(\frac{4\pi}{w}y)}{\pi w \sqrt{1 - (2y/w)^2}}, \quad (5)$$

where Γ is the reflection coefficient from the discontinuity and T is the wave amplitude of the transmitted wave. Also the functions $f_n(x)$ and $g_n(x)$ are the expansion modes used in the vicinity of the gap. k_m , a_0 , a_1 and a_2 are obtained through an infinite line analysis. This will involve solving a characteristic equation in a matrix form [9]. When the expansion functions are used in Eq. (1), followed by a Galerkin's procedure, the integral equation is converted into a set of linear equations which can be solved by a matrix inversion. The matrix elements are the reaction between different expansion modes. An example of a PWS mode and a traveling mode reaction is illustrated here.

$$Z_{self}^n = \int_{-\infty}^{\infty} \int_{-\infty}^{\infty} \bar{G}_{xx}(\lambda_x, \lambda_y) F_1^2(\lambda_y) P_1(\lambda_x) A_1(\lambda_x) e^{jnd_1 \lambda_x} d\lambda_x d\lambda_y, \quad (6)$$

where

$$F_1(\lambda_y) = \sum_{k=0}^2 \frac{a_k}{2} [J_0(\frac{w_1}{2}\lambda_y + k\pi) + J_0(\frac{w_1}{2}\lambda_y - k\pi)] \quad (7)$$

$$P_1(\lambda_x) = [e^{\frac{-j\lambda_x \pi}{2k_m}} + j] \int_{-\infty}^0 \sin k_m x e^{j\lambda_x x} dx, \quad (8)$$

$A_1(\lambda_x)$ is the Fourier transform of a PWS mode and d_1 is the half length of a PWS mode. Further asymptotic analysis has been applied to insure the convergence of the double infinite integrations.

IV. Results and discussions

MIC discontinuities are usually characterized by their equivalent circuits. Therefore, in order that the characterization be useful, all the disturbances on the current should die out quickly as one moves away from the discontinuity. In microstrip structures, any discontinuities will generate radiation and surface waves. These waves will also interfere with the microstrip line fundamental mode. Therefore, when radiation or surface waves are strong enough such that their interactions with the microstrip guided mode become noticeable over a significant distance from the discontinuities, the computed equivalent circuits will not be accurate. This implies that, for this case, if one tries to measure the equivalent circuits, the results will be different at different reference planes. Generally speaking, when the radiation and surface wave losses are less than 10% of the incident power, the computed results can be accurate within a few percent.

The equivalent circuit of a microstrip open end is computed from the reflection coefficient, which is obtained directly from the matrix inversion. Typical, 19 PWS modes of size 0.06 guided wavelength (0.6 guided wavelength in total) are used in the computation. The validity of this analysis is checked with the quasi-static method at low frequency. Fig. 4 shows the comparison between this analysis and the quasi-static method for a single layer case. The substrate thickness is $0.01\lambda_0$, which is thin enough to insure the accuracy

of the quasi-static method. The comparison yields very good agreement.

Energy loss due to radiation and surface waves at a microstrip open end is shown in Fig. 5 with and without a cover layer. The microstrip line in this case is embedded in between the substrate and the superstrate. It is found that with the presence of a cover layer, the loss increases with the increase of the superstrate dielectric constant due to stronger surface waves or radiation. The length extension (or capacitance) at the open end is shown in Fig. 6 for the same parameters as those in Fig. 5. It is found, by adding a cover layer, the excess length to substrate thickness ratio (or end capacitance) is larger due to stronger fringing field. In general, the excess length increases with the increase of effective dielectric constant and is insensitive to frequency except when the surface waves and/or radiation are strong.

For the gap case, after a matrix inversion is performed, the reflection coefficient Γ and the transmission coefficient T are S_{11} and S_{12} respectively. Therefore, the admittance matrix can be obtained through the following transformation

$$[Y] = ([U] - [S])([U] + [S])^{-1} \quad (9)$$

where $[U]$ is a unitary matrix. By comparison the two-port π network in Fig. 3, one finds

$$\frac{G_p + j\omega C_p}{G_0} = Y_{11} - Y_{12} \quad (10)$$

and

$$\frac{G_g + j\omega C_g}{G_0} = Y_{12} \quad (11)$$

The results of the gap discontinuity is compared with those by quasi-static [4] and measurements [12], and are shown in Fig. 7. Since the gap capacitance is small and is sensitive to device tolerances, the measurement has inherently difficulty. In this analysis, the frequency is chosen as 5 GHz. It is found that this dynamic model agrees well with both measurement and the quasi-static approach. Some discrepancies for large gap spacing may be due the fact that in such cases, the amount of energy coupled through the gap is comparable to the energy lost due to surface waves and radiation, and this aspect is not included in the quasi-static approach. The normalized gap capacitances C_g/w and C_p/w are shown in Figs. 8 and 9, respectively, for the same material arrangements as those shown in Fig. 5. It is found that the cover layer (superstrate) will increase both conductance and capacitance due to stronger fringing field and more energy losses. Also since $(G_p + j\omega C_p)$ is the input admittance when a perfect magnetic wall is in the middle of the gap, it is expected that due to image cancellation, G_g will be much larger than G_p . For narrower gap, C_g will be larger than C_p due to stronger end coupling. However for wide gap spacing, the input admittance seen at either side of the gap is mainly the open-end admittance, so C_p will be larger than C_g .

References

- [1] K. G. Gupta, R. Garg, and I. J. Bahl, *Microstrip lines and slotlines*. Dedham, MA: Artech House, 1979.
- [2] P. Benedek and P. Silvester, "Equivalent capacitance of microstrip open circuit," *IEEE Trans. on Microwave Theory and Technique*, Vol. MTT-20, pp. 511-516, May 1972.
- [3] P. Benedek and P. Silvester, "Equivalent capacitance for microstrip gaps and steps," *IEEE Trans. on Microwave Theory and Technique*, Vol. MTT-20, pp. 729-733, Nov. 1972.
- [4] M. Maeda, "An analysis of gap in microstrip transmission line," *IEEE Trans. on Microwave Theory and Technique*, Vol. MTT-20, pp. 390-396, April 1972.
- [5] R. H. Jansen, "Hybrid mode analysis of end effects of planar microwave and millimeter wave transmission line", *Proc. IEE, pt. H*, vol. 128, pp. 77-86, 1981.
- [6] R.H. Jansen, "The spectral domain analysis for microwave integrated circuits (Invited Paper)," *IEEE Trans. on Microwave Theory and Technique*, Vol. MTT-33, no. 10, pp. 1043-1056, Oct. 1985.
- [7] P. B. Katehi and N. G. Alexopoulos, "Frequency-dependent characteristics of microstrip discontinuities in millimeter wave integrated circuits," *IEEE Trans. on Microwave Theory and Technique*, vol. MTT-33, no. 10, pp. 1029-1035, Oct. 1985.
- [8] R. W. Jackson and D. M. Pozar, "Full wave analysis of microstrip open-end and gap discontinuities," *IEEE Trans. on Microwave Theory and Technique*, vol. MTT-33, no. 10, pp. 1036-1042, Oct. 1985.
- [9] O. Fordham, *Two layer microstrip transmission lines*, Master Thesis, UCLA 1987.
- [10] E.J. Denlinger, "A frequency dependent solution for microstrip transmission lines," *IEEE Trans. on Microwave Theory and Technique*, Vol. MTT-19, no. 1, pp. 30-39, Jan. 1971.
- [11] N.G. Alexopoulos and D.R. Jackson, "fundamental superstrate(cover) effects on printed circuit antennas," *IEEE Trans. on Antennas and Propagation*, Vol. AP-32, no. 8, pp. 807-816, Aug. 1984.
- [12] *The microwave Engineer's Handbook and Buyers' Guide*. New York: Horizon House, p. 72, Feb. 1969.

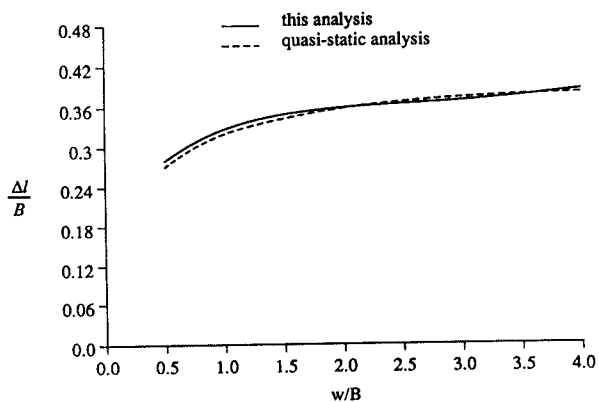


Figure 4. Excess length of an open-end microstrip line versus microstrip width.
 $\epsilon_r = 9.6$ and $B = 0.01 \lambda_0$.

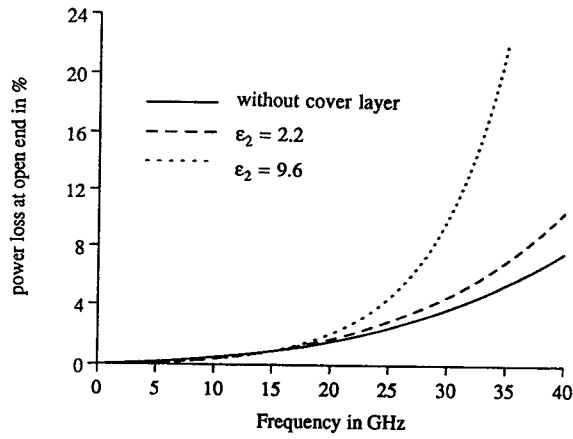


Figure 5. Energy loss at microstrip open end versus frequency.

$\epsilon_1 = 9.6$, $B = 0.3$ mm, $w = B$ and $t = B$.

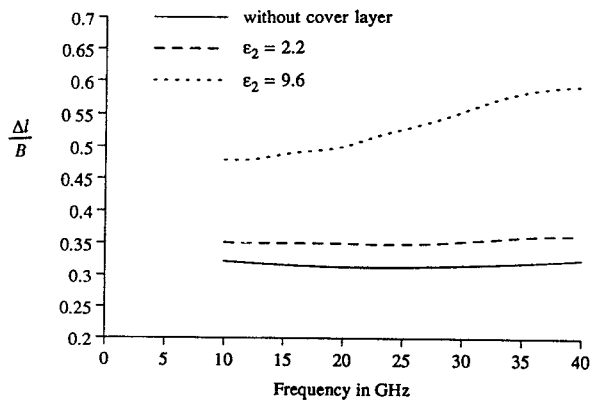


Figure 6. Excess length of an open-end microstrip line versus frequency.

$\epsilon_1 = 9.6$, $B = 0.3$ mm, $w = B$ and $t = B$.

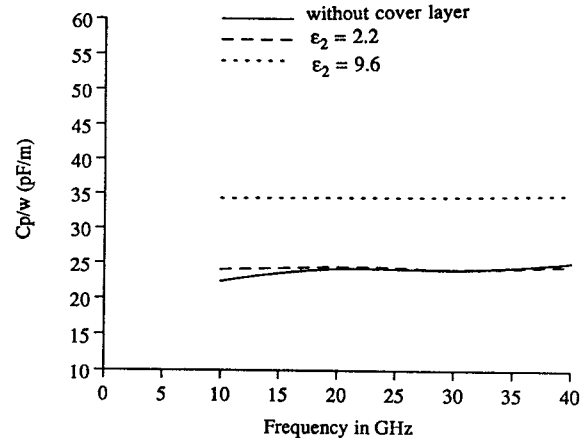


Figure 8. Normalized capacitance C_p/w versus frequency.

$\epsilon_1 = 9.6$, $B = 0.3$ mm, $w = B$, $t = B$ and $s = 0.3762 B$.

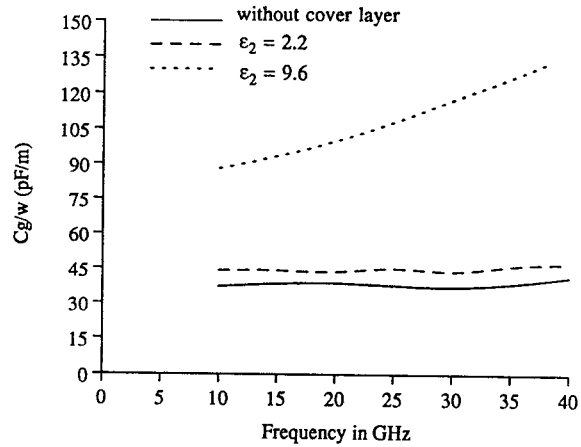


Figure 9. Normalized capacitance C_g/w versus frequency.

$\epsilon_1 = 9.6$, $B = 0.3$ mm, $w = B$, $t = B$ and $s = 0.3762 B$.

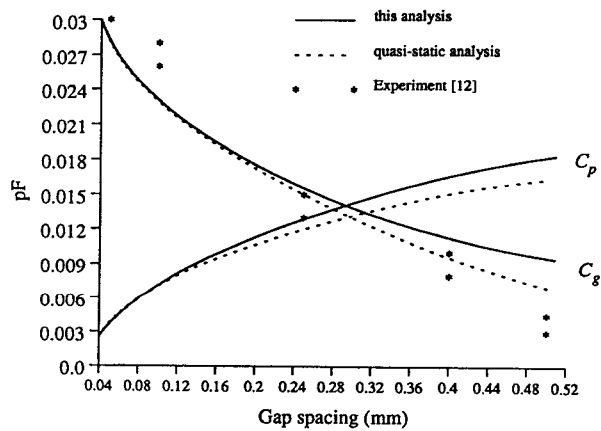


Figure 7. Gap capacitances versus gap spacing.

$\epsilon_1 = 8.875$, $\epsilon_2 = 1$, $B = 0.508$ mm and $w = B$.